ADVANCES IN ATMOSPHERIC SCIENCES, VOL. 25, NO. 4, 2008, 585–596

Effect of Chlorophyll-a Spatial Distribution on Upper Ocean Temperature in the Central and Eastern Equatorial Pacific

LIN Pengfei[1,2] (林鹏飞), LIU Hailong*[1] (刘海龙), and ZHANG Xuehong[1] (张学洪)

[1] *State Key Laboratory of Numerical Modeling for Atmospheric Sciences and Geophysical Fluid Dynamics, Institute of Atmospheric Physics, Chinese Academy of Sciences, Beijing* 100029

[2] *Graduate University of Chinese Academy of Sciences, Beijing* 100049

(Received 16 May 2007; revised 14 January 2008)

ABSTRACT

Effect of the spatial distributions of chlorophyll-a concentration on upper ocean temperature and currents in the equatorial Pacific is investigated through a set of numerical experiments by using an ocean general circulation model. This study indicates that enhanced meridional gradient of chlorophyll-a between the equator and off-equatorial regions can strengthen zonal circulation and lead to a decrease in equatorial sea surface temperature (SST). However, the circulation changes by themselves are not effective enough to affect SST in the equatorial cold tongue (CT) region. The comparison between the experiments indicates that the CT SST are more sensitive to chlorophyll-a distribution away from the equator. The off-equatorial chlorophyll-a traps more solar radiation in the mixed layer, therefore, the temperature in the thermocline decreases. The cold water can then be transported to the equator by the meridional circulation within the mixed layer. Furthermore, the relation among CT SST, the surface heat flux, and the equatorial upwelling are discussed. The study implies the simulation biases of temperature on the equator are not only related to the local ocean dynamics but also related to some deficiency in simulating off-equatorial processes.

Key words: sea surface temperature, the equatorial cold tongue, chlorophyll-a

DOI: 10.1007/s00376-008-0585-4

1. Introduction

About 58% of net surface solar radiation is absorbed by the seawater within the upper 1–2 m, the surplus can penetrate more deeply. The solar radiation penetration depth in clear seawater is considered to be constant. However, in reality, solar radiation penetration depth in the upper ocean presents spatial and temporal variations which are mainly influenced by the phytoplankton. The changes of chlorophyll-a concentration, which represents the amount of phytoplankton, can significantly modify radiation heating in the mixed layer and directly affect the ocean temperature (Lewis et al., 1990; Sathyendranath et al., 1991; Siegel et al., 1995; Ohlmann et al., 1998; Strutton and Chavez, 2004). The responses of ocean temperature and currents were studied in the oceanic general circulation models (Nakamoto et al., 2001; Murtugudde et al., 2002; Sweeney et al., 2005). Such fluctuation of ocean temperature and currents will also induce the changes in atmospheric circulation and further influence the whole global climate system (Timmermann and Jin, 2002; Miller, 2003; Gildor et al., 2003; Shell et al., 2003; Manizza et al., 2005; Marzeion et al., 2005; Wetzel et al., 2006; Ballabrera-Poy et al., 2007).

Chlorophyll-a concentration in the central and eastern equatorial Pacific is larger than that in the subtropical ocean because more nutrients are transported vertically by the upwelling at the equator. According to previous simulation results, the temperatures in the central and eastern equatorial Pacific were sensitive to the changes in chlorophyll-a concentration. Using an isopycnal ocean general circulation model (OGCM), Nakamoto et al. (2001) showed sea surface temperatures (SSTs) decreased by about 2°C in the equatorial Pacific when comparing space-time-varying attenuation depth based on chlorophyll-a concentration with a constant attenuation depth of 23 m.

*Corresponding author: LIU Hailong, lhl@lasg.ac.cn

While Murtugudde et al. (2002) found that the SSTs increased by about 1°C in the same region by comparing spatial varying penetration depth with constant depth of 17 m in a coordinate reduced gravity OGCM. Whether SSTs in the eastern equatorial Pacific decreased or increased, the magnitudes of SST variations mentioned above are still comparable to those of interannual anomalies. Thus, clarifying the effect of chlorophyll-a concentration distribution and its variation on the structures of upper ocean temperature and current will help us to better understand the variations of SST in the equatorial Pacific Ocean, especially in the cold tongue (CT) region.

The CT is one of the most persistent and intense regions of heat gain, but the SSTs in the region are lowest at the same latitude. This indicates that upwelling, vertical mixing and other ocean dynamical processes are the main factors controlling both the mean state and variations of CT SST. The distribution and variation of chlorophyll-a concentration can affect ocean temperatures through direct heating or altering stratification. Sweeney et al. (2005) and Lin et al. (2007) pointed out definitively that the increase in chlorophyll-a concentration might lead to the decrease in SST due to strengthening of the equatorial upwelling. Therefore, it is ocean dynamics processes that determine the response of CT SST to chlorophyll-a concentration.

Upwelling in the equatorial Pacific, together with the poleward Ekman transport, the subduction in the mid-latitudes, and the equatorward flow in the thermocline consist of a meridional circulation. The change in equatorial SST may not only relate to local physical processes but also to off-equatorial temperature and current. Sweeney et al. (2005) indicated that there were two possible off-equatorial processes which can affect CT SST. First, an increase in penetration depth deepens the mixed layer and decreases the poleward flow, and consequently weakens the equatorial upwelling. Second, an increase in penetration depth warmed the temperature in the thermocline off the equator and the warm temperature anomaly could be transported to the equator through the equatorwards circulation at the base of the mixed layer and could then warm the CT SST.

According to our previous studies (Lin et al., 2007), if only increasing the chlorophyll-a concentration on the equator, the magnitude of SST cooling was only about 0.2°C, just one half of the difference in SST between the sensitive (considering the spatial distribution of chlorophyll-a concentration) and control (a constant penetration depth) runs. In addition, there was consistent cooling in the deeper layers between the equator and off-equatorial regions associating with two maximal cooling centers around 10° on both sides of the equator. At the same time, there were two strong anomalous meridional circulations in the upper layer. These two off-equatorial processes can be important in affecting equatorial SST. However, it is unclear which process is more effective in doing so. Thus, the relationships between the variations of off-equatorial processes and equatorial SST will be focused on in this paper.

Accompanied by the above issues, a set of sensitive experiments are conducted by using an ocean general circulation model. The effects of equatorial and off-equatorial horizontal distribution of chlorophyll-a concentration on equatorial temperature and current are compared respectively. The model and designed experiments are introduced in section 2. Section 3 presents the results. Section 4 and 5 are discussions and conclusions, respectively.

2. Model and experiments

In this paper, LASG/IAP (State Key Laboratory of Numerical Modeling for Atmospheric Sciences and Geophysical Fluid Dynamics/Institute of Atmospheric Physics) Climate System Ocean Model (LICOM, Zhang et al., 2003; Liu et al., 2004a,b) is employed. The model resolution is 1° in the zonal direction and resolution varies from (1/4)° at the equator to 1° poleward in the meridional direction. The model has 30 vertical layers with the 15 layers in the top 150 m. The details of the vertical grid distribution can be found in Wu et al. (2005).

The surface boundary condition of temperature takes the form of observed net surface heat flux plus a Newton cooling term. Wind stress, heat flux and a coupling coefficient are from MPI-OMIP (Röske, 2001) derived from ERA-15 (Gibson et al., 1997). The SST and sea surface salinity (SSS) are restored to their observed values from WOA98 (World Ocean Atlas 98, http://www.nodc.noaa.gov/) data. Pacanowski and Philander's (1981) scheme for the vertical mixing is employed in the model. The Gent and McWilliam's (1990) scheme is also used for parameterizing the effects of mesoscale eddies. The Laplacian form horizontal viscosity is chosen with a constant viscosity coefficient of 20000 $m^2\ s^{-1}$.

A two-exponential formula is used to parameterize solar radiation penetration.

$$I = I_0 \times (R_1 e^{-K_1 Z} + R_2 e^{-K_2 Z}) , \qquad (1)$$

where I is the downwelling shortwave radiation penetrating a certain depth Z and I_0 is the net downwelling radiation under the sea surface. The R_1 and $1/K_1$

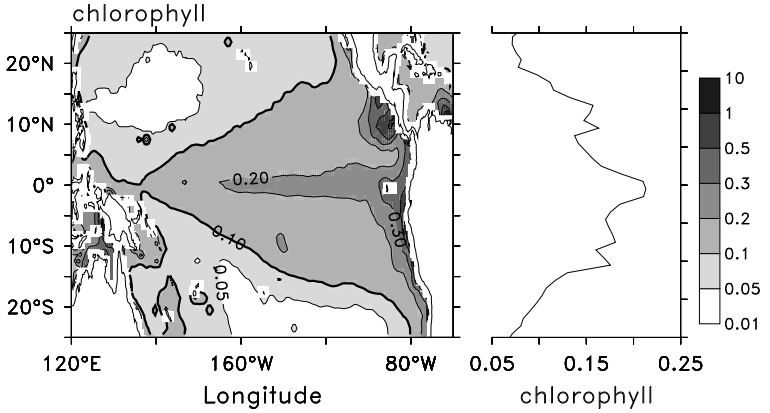

Fig. 1. The annual mean chlorophyll-a concentration of the SeaWiFs (units: mg m^{-3}, left panel) and its zonal mean from 130°E to 80°W (right panel). The thick dotted curve represents the chlorophyll-a concentration of 0.1 mg m^{-3}.

represent the fraction of the total solar flux that resides in the infrared band and its penetration depth, respectively. The R_2 and $1/K_2$ represent parameters in the ultraviolet and visible bands. In LICOM, the solar radiation penetration scheme of Paulson and Simpson (1977, hereafter PS77) was employed. Based on Jerlov's (1968) classification of water type, the seawater was assumed to be type I. Thus, $R_1 = 0.58, R_2 = 0.42, K_1 = 1/0.35$ m^{-1} and K_2=1/23.0 m^{-1} were taken. In order to describe the influence of chlorophyll-a concentration on the solar radiation penetration, Ohlmann's (2003, hereafter O03) scheme was used. Different from PS77, the R_i $(i = 1, 2)$ and $1/K_i$ $(i = 1, 2)$ in O03 scheme are all functions of chlorophyll-a concentration (C). R_i $(i = 1, 2)$ and $1/K_i$ $(i = 1, 2)$ can be found in Table 1 of Ohlmann (2003). Using the PS77 and O03 scheme, two experiments are conducted. These two experiments are referred to as the PS77 run and the O03 run, respectively.

At present, most OGCM used in climate system models have a vertical resolution of about 10 m in the upper ocean. The infrared radiation is almost entirely absorbed in the upper 1–2 m. The ultraviolet and visible radiation can penetrate below the mixed layer, so the change in absorbed energy in ultraviolet and visible bands is the determinative factor to be used in solar penetration schemes. Therefore, the effect of chlorophyll-a on the shortwave radiation in the sensitive experiments is mainly represented by changing the e-folding depth in the second term of Eq. (1).

The SeaWiFS observed chlorophyll-a concentration (Fig. 1) shows that the chlorophyll-a concentration exceeds 0.2 mg m^{-3} in the equatorial Pacific due to the upwelling driven by eastward trade winds. Outside the equator, except some regions in the off-equatorial western Pacific, chlorophyll-a concentration is also higher than 0.1 mg m^{-3} within 20° in the tropical Pacific. Using O03 scheme, the penetration e-folding depth of the 0.1 mg m^{-3} chlorophyll-a concentration approximately equals 17 m.

According to the observed spatial distribution of chlorophyll-a concentration, three sensitive experiments are designed. As mentioned above, only the e-folding attenuation depth of the visible and ultraviolet band (DVUB) in PS77 scheme is modified to mimic the spatial distribution of chlorophyll-a. In first experiment, which is referred to as Sen20D run, the DVUB has been set to 17 m within 20° of 130°E and 80°W. The other regions remain 23 m. Only the DVUB within 5° of 130°E and 80°W is set to 17 m in the second experiment. This run is referred to as the Sen5D run. In order to evaluate the effect of chlorophyll-a concentration distribution off the equator on equatorial temperature, the DVUB is set to 17 m outside 5° to 20° between 130°E and 80°W, and the depth in the other regions remains unchanged in the third experiment. This run is referred to as the Sen5D20D run. The rectangular frames of Fig. 2 show the regions where the DVUBs are modified.

All five experiments are driven by annual mean forcing in this paper, including wind stresses, surface heat fluxes and chlorophyll-a concentration. At first the model is run for 20 years from a motionless state using the PS77 scheme. Following this, the final state of the 10th year of the PS77 run is used as the initial conditions for the other four runs. The four integrations are all carried out for 10 years. The annual mean of the last year of the five experiments are analyzed to evaluate the effect of the annual mean spatial distribution of chlorophyll-a on SST at the equator. Table 1 summarizes all the information of the five experiments.

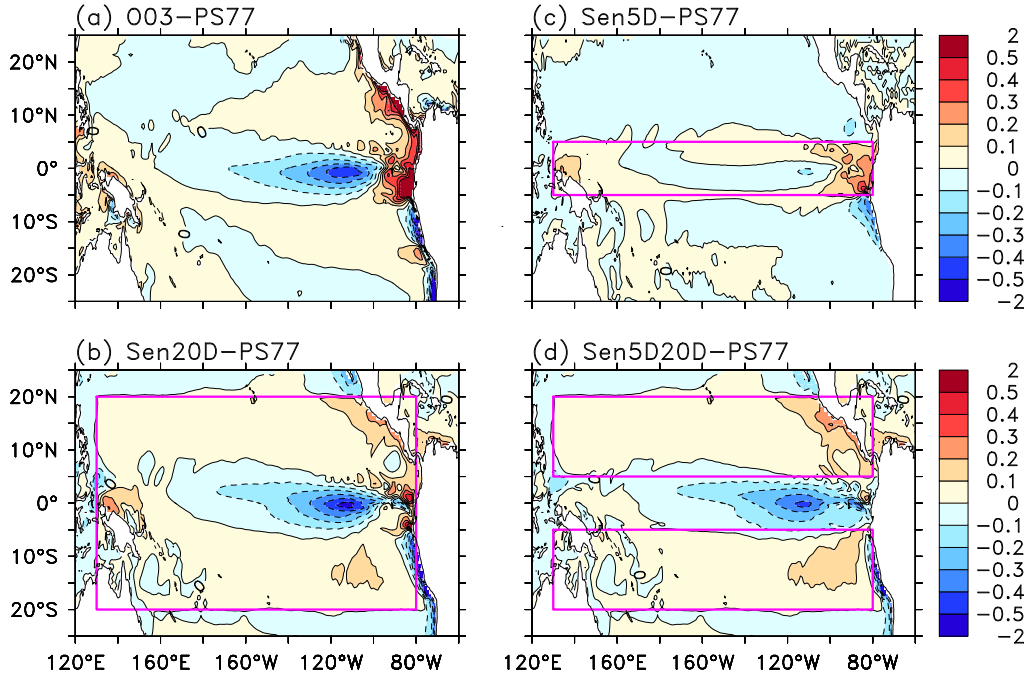

Fig. 2. The differences in sea surface temperature (°C) between the sensitive runs and the PS77 run. The purple rectangle boxes represent the region in which the e-folding penetration depth is changed from 23 m to 17 m.

Table 1. The configuration of all the experiments in the paper.

Names	Chlorophyll distribution and its domain	Initial values	Forcing fields	Integration time
PS77	Global penetration depth of 23 m	WOA98's temperature and salinity data from motionless	Annual mean MPI-OMIP data	20 years
O03	Annual mean SeaWiFs chlorophyll distribution	PS77 run in 10th year Dec	The same as above	10 years
Sen5D	Region(130°E–80°W, 5°S–5°N) depth of 17 m, others depth of 23 m	The same as above	The same as above	10 years
Sen20D	Region (130°E–80°W, 20°S–20°N) depth of 17 m, others depth of 23 m	The same as above	The same as above	10 years
Sen5D20D	Region (130°E–80°W, 5°–20°S), (130°E–80°W, 5°–20°N) depth of 17 m, others depth of 23 m	The same as above	The same as above	10 years

asymmetric meridional circulation in the tropical Pacific Ocean, the two cooling centers on both sides of the equator in the O03, Sen20D and Sen5D20D runs are asymmetric.

3. Results

3.1 *SST*

Figure 2 shows the differences in SST between the PS77 run and the other sensitive runs. There are negative anomaly centers of SST all around 110°W at the equator in the CT region. The differences in SST between the Sen20D, Sen5D20D and PS77 runs reach 0.5°C and 0.4°C, respectively, which are comparable to the differences in SST between O03 run and PS77 run. However their differences are more than double that between the Sen5D and PS77 run. The differences between the control and sensitive experiments indicate that spatial distribution of chlorophyll-a has an important influence on SST in the CT region. Moreover,

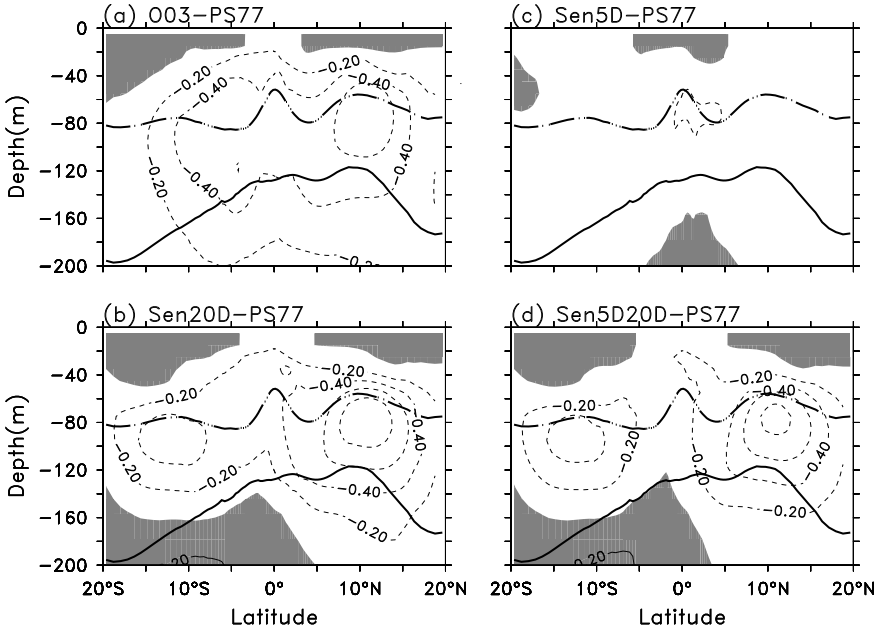

Fig. 3. The differences in zonal averaged temperature (°C) from 130°E to 80°W between the sensitive runs and the PS77 run. The positive values are shaded. The thick dash and thick solid curve represent the zonal averaged mixed layer depth (the depth at which the temperature is 0.5°C smaller than SST) and the thermocline depth (20°C isothermal line) in the PS77 run, respectively.

the effect of the off-equatorial chlorophyll-a on SST in the CT region is even larger than the effect of local chlorophyll-a distribution.

In addition, the magnitude and spatial structure of the differences in SST for Sen20D equal approximately the summation of the differences of the Sen5D and Sen5D20D runs. That indicates that the effects of equatorial and off-equatorial chlorophyll-a distribution on the CT SST are basically linear. However, the SST increases (decreases) when the e-folding penetration depth decreases (increases) in the region east of 90°W at the equator because heat budgets in that region are mainly controlled by the local surface heat flux.

3.2 *Zonal averaged temperature*

The differences in zonal averaged temperature between the PS77 run and the other sensitive runs are shown in Fig. 3. In the Sen5D run the cooling center just below the mixed layer is located at the equator and its magnitude is only 0.2°C. However, the two subsurface cooling centers are located around both northern and southern 10° in the other three runs. The maximum temperature differences exceed 0.8°C. The temperature decreases below the mixed layer are due to the decrease in penetration depth and therefore more heat is trapped in the upper mixed layer. In the O03, Sen20D and Sen5D20D runs, equatorial SST anomalies are closely related to the temperature anomalies below the mixed layer off the equator. Due to the

3.3 *Circulation*

The three dimensional structures of circulations are complex in the tropical Pacific. Besides the bands of zonal flowing currents: the westward South and North equatorial currents (SEC and NEC) and the eastward North Equatorial Countercurrent (NECC) and Equatorial Undercurrent (EUC), there are also meridional circulations near the equator. Figures 4, 5 and 6 show the differences of zonal, meridional and vertical currents between the PS77 run and the other sensitive runs respectively. It is different from the differences of zonal mean temperatures in that the main discrepancies of the currents lay between the Sen5D20D run and the other runs. The enhancement of SEC, EUC and upwelling in the O03, Sen5D and Sen20D runs leads to strengthening zonal circulation along the equator (Figs. 4 and 6). The meridional circulations in the mixed layer also accelerate (Fig. 5). However, the circulations in the Sen5D20D run are not obviously enhanced (Figs. 4, 5 and 6).

As pointed out by Lin et al. (2007), the chlorophyll-a concentration gradient between the equator and off-equatorial regions lead to the circulation change in the upper layer. When the chlorophyll-a distribution is

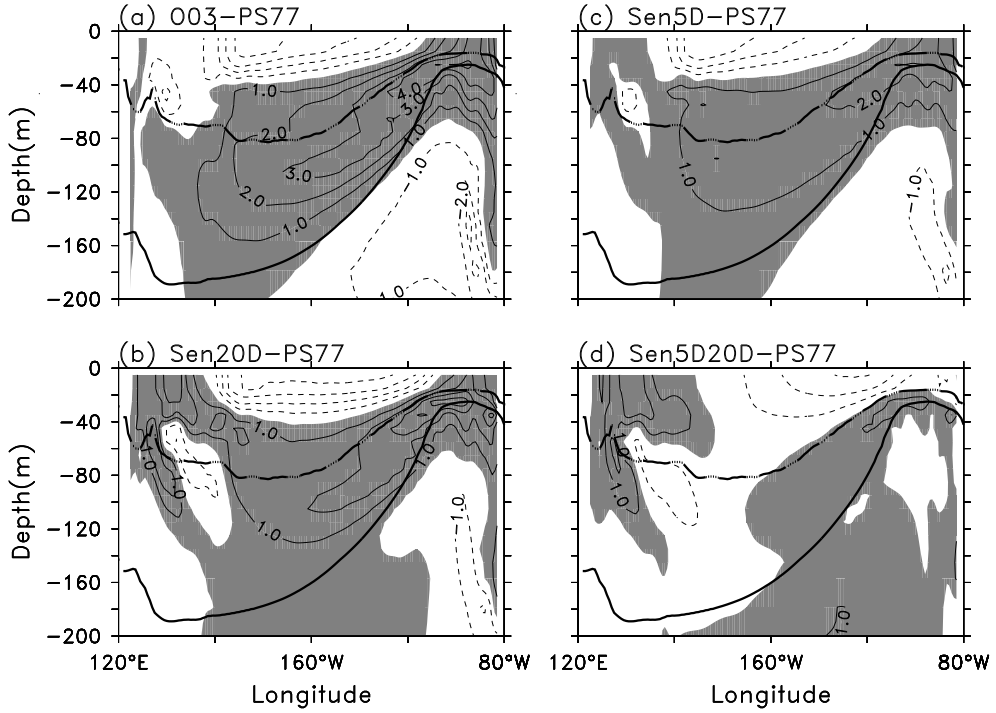

Fig. 4. Same as Fig. 3, except for the zonal current along the equator averaged from 1°S to 1°N (units: cm s^{-1}).

considered, the stratification in the upper layer along the equator will be enhanced due to more heat being trapped by the chlorophyll-a. That causes the mixed layer at the equator to become shallow and increases the meridional pressure gradient between the equator and off-equator regions. Therefore, the zonal currents are enhanced due to the geostrophic balance, and then the meridional and vertical currents do the same. Because the heating along the equator in the Sen5D20D run does not change, the circulation in this experiment are also close to the PS77 run.

3.4 *Meridional Heat Transport (MHT)*

Although the increase in the chlorophyll at the equator cause the enhancement of the tropical circulation (Figs. 4, 5 and 6), the SST in the CT region does not change much (Fig. 2). However, the large SST decrease in the CT region is mainly caused by the cold water below the mixed layer due to the increase in chlorophyll off the equator (Figs. 2 and 3). That suggests not only the enhancement of the equatorial upwelling but also that the cold subsurface water can lead to cold SST in the that region.

In order to distinguish the contributions of temperature and current anomalies to the MHT, the temperatures, T, and currents, v, in the sensitive runs are decomposed into the value of the PS77 run plus the value departure from the PS77 run. That can be written as

$$vT = (v_0 + v')(T_0 + T') \,,$$

where v_0 and T_0 are the temperature and current of the PS77 run and $v' = v - v_0$ and $T' = T - T_0$ are the temperature and current differences between sensitive runs and PS77 run.

After integrations and the arrangement, the formula becomes

$$\int_{X_E}^{X_W}(\int_{-H(x)}^{0}\rho c_p vTdz)dx - \int_{X_E}^{X_W}(\int_{-H(x)}^{0}\rho c_p v_0 T_0 dz)dx = \int_{X_E}^{X_W}(\int_{-H(x)}^{0}\rho c_p v_0 T' dz)dx + \int_{X_E}^{X_W}(\int_{-H(x)}^{0}\rho c_p v' T_0 dz)dx + \int_{X_E}^{X_W}(\int_{-H(x)}^{0}\rho c_p v' T' dz)dx \,, \quad (2)$$

where $\rho = 1.029 \times 10^3$ kg m^{-3} is the density of seawater and the $c_p = 3996$ J kg^{-1} K^{-1} is the specific heat at constant pressure. $-H(x)$ is the oceanic bottom. Although the calculation of MHT is integrated from the oceanic bottom to sea surface, the changes mainly occur in the upper layer. X_W and X_E represent the western and eastern boundary of the integration, respectively. Because the calculation about the MHT need satisfy, $\int_{X_E}^{X_W}(\int_{-H(x)}^{0} vdz)dx = 0$ the western coast of the Indian Ocean and the eastern coast

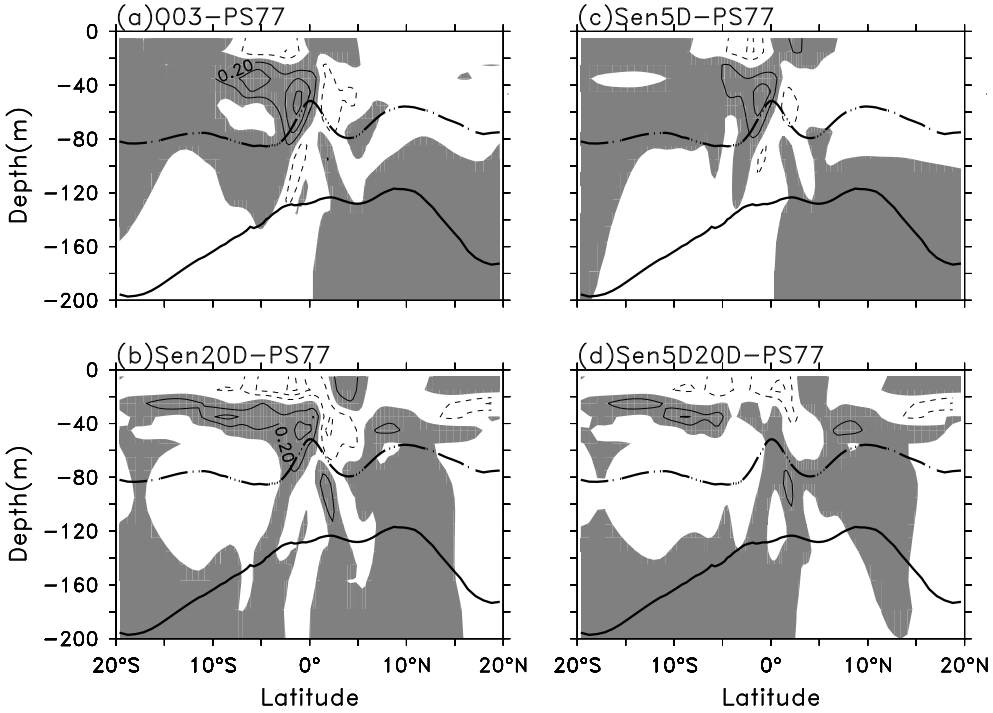

Fig. 5. Same as Fig. 3, except for the zonal averaged meridional currents from 130°E to 80°W (units: cm s^{-1}).

of the Pacific are taken as the western and eastern boundary, respectively. Since the penetration depths in the Sen5D, Sen20D and Sen5D20D runs are changed only in the Pacific, the changes in the MHT are caused by the differences in the Pacific.

According to preceding analysis, we know that the differences in zonal averaged temperature are mainly located in the upper 200 m (Fig. 3) and the current differences are mainly located in the upper 100 m (Fig. 5). Hence, the first two terms on the right side of formula (2) represent the transport of temperature anomalies in the thermocline by the mean meridional circulations and the transport of the mean temperature by the anomalous meridional circulations, respectively. Because the magnitude of the third term on the right side of Eq. (2) is at least one order smaller than the others, it is not discussed any more and is also not shown in Fig. 7.

Figure 7 shows the differences in MHT between the sensitive runs and the PS77 run according to Eq. (2). The poleward MHTs in the O03, Sen20D and Sen5D20D runs increase relative to those in the PS77 run. The magnitudes of their variations are about 0.04 PW (1 PW=1×10^{15} W) and larger in the Northern Hemisphere than those in the Southern Hemisphere. The increase in the MHT is mainly limited to within 4° of latitude in the Sen5D run. While in the regions outside 4°, the MHT slows down and its variation is about 0.01 PW, smaller than those of other runs. When further comparing the differences of the first two terms on the right sides in the Eq. (2) in the other sensitive runs, it is found that the acceleration of the MHT is attributed to the transport of temperature anomalies in the thermocline by mean current (the first term) in the O03 and Sen5D runs, while the current variations in the mixed layer (the second term) weakened the MHT.

The MHT difference in the Sen20D run is similar to that in the Sen5D20D run. From the equator to 5°N in the Northern Hemisphere, the MHT differences in the Sen20D and Sen5D20D runs are almost consistent with those in the Sen5D and O03 runs. Their MHT differences of the first term on the right side of Eq. (2) can approach 0.08 PW, which is comparable to that in the O03 run. Nevertheless, the results in the Southern Hemisphere are opposite to those in the Northern Hemisphere. The second term on the right side of formula (2) leads to the MHT increase while the first term results in the MHT decrease. Whatever the differences in MHT are, the transports of temperature anomalies in the thermocline by mean currents influence the acceleration of the MHT. This also illuminates that off-equatorial processes play important roles in the variations of equatorial temperature.

There are warm temperature anomalies under the 160 m level in the Southern Hemisphere from the dif-

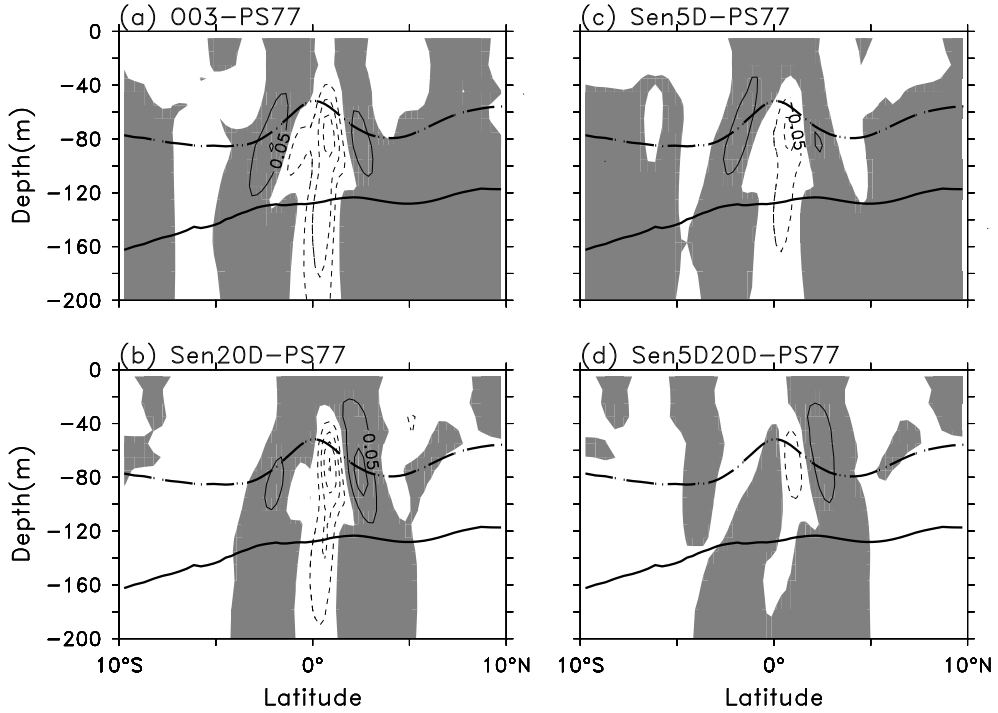

Fig. 6. Same as Fig. 3, except for the zonal averaged vertical velocity from 130°E to 80°W (units: m d^{-1}).

ferences in zonal averaged temperatures in the Sen20D and Sen5D20D runs (Fig. 3). These structures of warm anomalies are different from those in the other runs. Their central values can reach about 0.2°C. The warm anomalies under the thermocline reduce the temperature contrast between the mixed layer and thermocline and consequently weaken the poleward MHT in the Southern Hemisphere. This can explain why the MHT differences in the Sen20D and Sen5D20D runs are asymmetric in the Northern and Southern Hemisphere. The occurrence of warm anomalies under the thermocline may be related to the boundary around 20°S set up in these two runs.

4. Discussion

In this paper, the impacts of the equatorial and off-equatorial chlorophyll-a concentration distribution on the temperatures in the Pacific CT are investigated through comparing the results of sensitive experiments. The temperature variations in the CT are not only a simple response to the surface heat flux but also influenced by the local upwelling and vertical mixing which include the off-equatorial effects. In order to better understand the processes that control the SST in the Pacific CT region, an idealized model is proposed.

In the stand-alone OGCM, without considering the effects of the horizontal advections and mixing, the temperature variations in the mixed layer are approximately balanced by the surface heat flux and vertical advections in the Pacific cold tongue. The equation for the temperature variations can be written as:

$$\frac{\partial T}{\partial t} = \frac{Q_0 - Q_{-H}}{\rho c_p H} - \frac{W}{H}(T - T_\mathrm{b}) \,, \tag{3}$$

where Q_0 is the surface net heat flux and Q_{-H} is the shortwave radiation penetrating the mixed layer. H is mean mixed layer depth, W and T_b are the vertical velocity and temperature at the base of mixed layer, respectively. ρ is the density of seawater and c_p is the specific heat. Supposing Q_0, Q_{-H}, H, W and T_b are kept constant, Eq. (3) can be further simplified as

$$\frac{\partial T}{\partial t} + AT = B \,, \tag{4}$$

where

$$A = \frac{W}{H} \text{ and } B = \frac{Q_0 - Q_{-H}}{\rho c_p H} + \frac{W}{H} T_\mathrm{b} \,.$$

The former indicates the e-folding time scales of temperature variations, while the latter represents heating rate in the mixed layer caused by the heat flux and vertical upwelling. Through solving (seeking) the solution of Eq. (4), the solution takes the form of

$$T(t) = (T_0 - T_\mathrm{E})e^{-At} + T_\mathrm{E} \,,$$

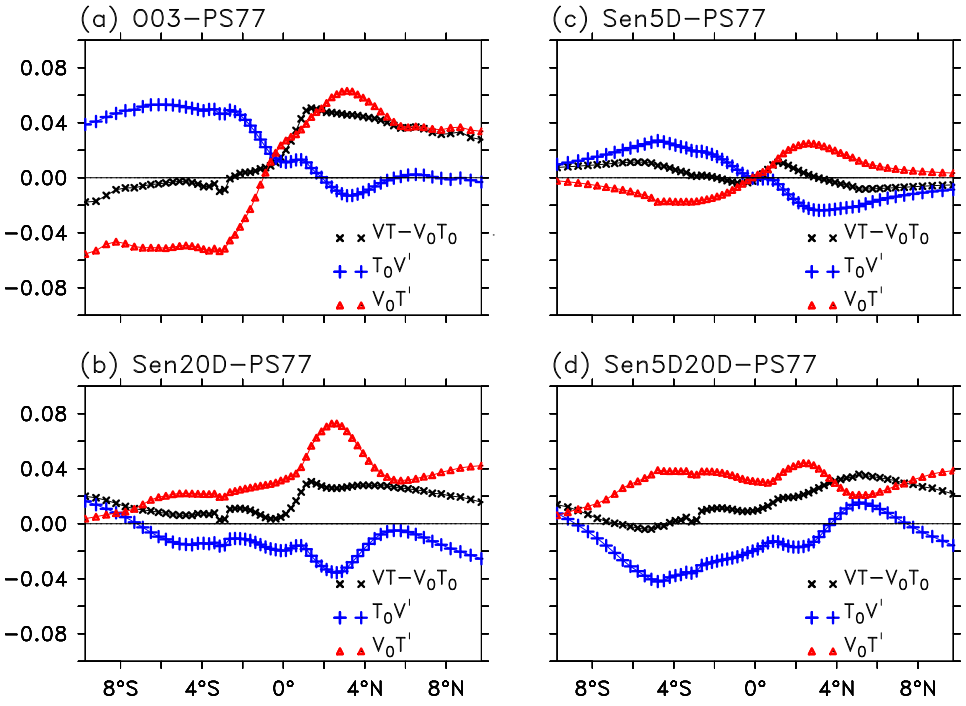

Fig. 7. The differences in the meridional heat transport (MHT) between the sensitive runs and the PS77 run (black line adding ×), the MHT due to meridional current anomalies (blue line adding +) and the MHT due to temperature anomalies (red line adding △). units: PW (1 PW=1×10^{15} W).

where

$$T_{\rm E} = \frac{B}{A} = \frac{Q_0 - Q_{-H}}{\rho c_p H}\frac{H}{W} + T_{\rm b}\ ,$$

and T_0 is an initial temperature. When t approaches infinity, $T(t)$ tends to the equilibrium temperature ($T_{\rm E}$) in the mixed layer. $T_{\rm E}$ is not only related to the surface heat flux and penetrative radiation, but is also influenced by vertical upwelling and the temperature at the base of mixed layer.

The first term of solution $T_{\rm E}$ (denoted as $T_{\rm E1}$) represents the temperature variations in the e-folding time scales due to the surface heat flux and shortwave penetration. The magnitude of this term can be estimated using the PS77 scheme. The shortwave radiation in the CT region is about 220 W m^{-2}. If the e-folding penetration depth in the visible and ultraviolet bands is 17 m, Q_{-H} (17 m)=28 W m^{-2}. Similarly, if penetration depth is 23 m, Q_{-H} (23 m)=39 W m^{-2}. Given Q_0=150 W m^{-2}, ρ=1029 kg m^{-3}, c_p = 3996 J kg^{-1} K^{-1}, W=1 m d^{-1} and H = 20 m, $T_{\rm E1}$ can be estimated as 2.6°C and 2.4°C when the penetrative depths are 17 m and 23 m, respectively. If $T_{\rm b}$ is kept fixed and only the heat flux changed, mean SST in the CT would increase by 0.2°C when the e-folding penetration depth varies from 23 m to 17 m. This magnitude is close to the results of the sensitive experiments.

The aforementioned discussions are in the case of keeping $T_{\rm b}$ unchanged. However, the changes in the local heat flux and off-equatorial temperature anomalies, which can be transported by mean meridional currents, can both lead to $T_{\rm b}$ change. Considering the local effect of decrease in shortwave radiation at the base of the local mixed layer, assuming the depth of the subsurface layer is 20 m, the decrease in $T_{\rm b}$ resulting from the decrease in shortwave radiation equals the magnitude of the temperature increase in the surface layer, and its value is about 0.2°C. That means the warm tendency of temperature in the mixed layer would be suppressed when considering the decrease in shortwave radiation under the local mixed layer.

Besides the local decrease in shortwave radiation under the mixed layer, the effect of transport of temperature anomalies from off-equatorial regions is another important factor resulting in a decrease in SST at the equator. Through the above sensitive experiments, it is found that $T_{\rm b}$ has been changed significantly. Moreover, the magnitude of decrease in temperature (reaching 0.5°C in Fig. 3) in the thermocline off the equator exceeds that due to the decrease in shortwave radiation at the base of mixed layer. It is estimated that the cold advection off the equator can lead to a decrease in temperature by about 0.3°C. By comparing the results in the Sen5D20D run with those

in the Sen5D run, the importance of the transport of off-equatorial temperature anomalies on equatorial SST variation is also confirmed.

Sweeney et al. (2005) and Lin et al. (2007) have pointed out that the decrease in penetration depth at the equator can lead to the changes in the heating gradient between the equator and off-equatorial regions and can then strengthen the equatorial ocean circulations. According to the expression of T_{E1}, the enhancement of W would itself result in a decrease in the magnitude of temperature increase. For instance, when W=2 m d^{-1}, the magnitude is reduced to 0.1°C. That means if W at the equator increases, the magnitude of SST increase would be reduced to some extent. In the Sen5D run, the decrease in penetration depth within 5° of latitude would result in an increase in upwelling at the equator and then cause SST to decrease. Comparing the SST and circulations in the Sen5D run with those in the Sen5D20D run, although upwelling in the former is larger than one in the latter, the magnitude of SST decrease is more obvious in the latter. This indicates that the effect of temperature variation in the thermocline off the equator on equatorial SST is more important than that of pure upwelling on the equator.

During the process of the above derivation, SST tends to reach the equilibrium state in the form of e-exponential. According to the above characteristic values, the e-folding time scale is estimated to be about 20 days. In the OGCM experiments, especially in the O03, Sen20D and Sen5D runs, SST in the CT turned warmer first and then colder (Lin et al., 2007). The processes result from the interactions among the heat flux, upwelling and temperature anomalies in the thermocline. Relative to local upwelling and the transport of off-equatorial temperature anomalies in the thermocline, the heating effect of heat flux is the most direct mechanism causing temperature to increase. However, accompanied by the response of the circulation to the change in temperature structures, the effect of upwelling and the transport of off-equatorial temperature anomalies on equatorial SST emerges gradually.

Based on the analysis of sensitive experiments and a simplified model, it is found that the change in SST in the Pacific CT is dominated mainly by ocean dynamics. The climatic mean state of the CT is influenced more by the transport of off-equatorial temperature anomalies in the thermocline. The studies of Lengaigne et al. (2007) and Anderson et al. (2007) also indicated that the distribution of chlorophyll-a off the equator can affect the temperature in the Pacific CT. Anderson et al. (2007) pointed out that chlorophyll-a concentration can cause the maintenance of the CT. The regions most responsible for affecting the temperature were located off the equator. Thus, the distribution of chlorophyll-a off the equator is crucial regarding its influence the change in mean CT temperature.

There are still many unresolved problems in simulating the tropical Pacific. For example, the cold tongue is too strong and extends too far west in the models, etc. (Mechoso et al., 1995; Latif, 2001; Davey, 2002). From this study, the simulation biases at the equator may not only be related to local ocean dynamics but also related to the simulation biases of some off-equatorial processes.

5. Conclusions

In this paper, the effects of chlorophyll horizontal spatial distribution on upper ocean temperature and current in the tropical Pacific are investigated through comparing the results of sensitive experiments using an OGCM. In particular, we explore how off-equatorial chlorophyll distribution impacts the SST in the CT region.

The increase in the meridional gradient of chlorophyll-a distribution between the equator and off-equatorial regions can strengthen the SEC (about 4 cm s^{-1}), EUC (about 2 cm s^{-1}) and upwelling significantly. Meanwhile, poleward divergence in the mixed layer and equatorward convergence at the base of mixed layer also strengthen. However, the effect of variation of circulations on the mean SST in the CT is not very effective.

The comparisons of different experiments suggested that the change in SST in the Pacific CT region is more sensitive to off-equatorial chlorophyll-a distribution than equatorial chlorophyll-a distribution. Through decomposing the meridional heat transport, we found that off-equatorial chlorophyll distribution can lead to temperature anomalies in the thermocline. The anomalies can then be transported to the equator by the meridional circulation in the mixed layer.

Based on a simple model, we also confirm that the temperature variation in the thermocline off the equator plays an important role in equatorial SST variation. Although the increase in radiative heating is the most direct process resulting in an increase in temperature, the effect of upwelling and off-equatorial transport of temperature anomalies on equatorial SST emerges gradually, accompanied by a response of the circulation variation to the changes in temperature structures.

The discussion is just based on a stand-alone ocean model. However, there is not only the response of heat flux to SST variation, but also the response of surface wind to the variation of SST gradient in the coupled ocean-atmosphere system. How the SST in the Pacific

CT region changes in a coupled model needs further investigation.

Acknowledgements. This study is jointly supported by the National Natural Science Foundation of China under Grant Nos. 40233031, 40375030, 40405017, 40523001 and 40775054, the National Key Programme 2006CB403600, the Chinese Academy of Sciences (CAS) International Partnership Creative Group "The Climate System Model Development and Application Studies". The authors would like to thank the anonymous reviews for their valuable comments and suggestions.

REFERENCES

Anderson, W. G., A. Gnanadesikan, R. Hallberg, J. Dunne, and B. L. Samuels, 2007: Impact of ocean color on the maintenance of the Pacific Cold Tongue. *Geophys. Res. Lett.*, **34**, L11609, doi: 10.1029/2007GL030100.

Ballabrera-Poy, J., R. Murtugudde, R. H. Zhang, and A. J. Busalacchi, 2007: Coupled ocean-atmosphere response to seasonal modulation of ocean color: Impact on interannual climate simulations in the Tropical Pacific. *J. Climate*, **20**, 353–374.

Davey, M. K., and Coauthors, 2002: STOIC: A study of coupled model climatology and variability in tropical ocean regions. *Climate Dyn.*, **18**, 403–420.

Gent, P. R., and J. C. McWilliams, 1990: Isopycnal mixing in ocean circulation models. *J. Phys. Oceanogr.*, **20**, 150–155.

Gibson, J. K., P. Kållberg, S. Uppala, A. Hernandez, A. Nomura, and E. Serrano, 1997: ERA description. *ECMWF Reanalysis Project Report Series*, No. 1, European Centre for Medium-Range Weather Forecasts, Reading, 72pp.

Gildor, H., A. H. Sobel, M. A. Cane, and R. N. Sambrotto, 2003: A role for ocean biota in tropical intraseasonal atmospheric variability. *Geophys. Res. Lett.*, **30**, 1460, doi: 10.1029/2002GL016759.

Jerlov, N. G., 1968: *Optical Oceanography*. Elsevier Press, 194pp.

Latif, M., K., and Coauthors, 2001: ENSIP: the El Niño simulation intercomparison project. *Climate Dyn.*, **18**, 255–276.

Lengaigne, M., C. Menkes, O. Aumont, T. Gorgues, L. Bopp, J. M. Andre, and G. Madec, 2007: Influence of the oceanic biology on the tropical Pacific climate in a coupled general circulation model. *Climate Dyn.*, **28**, 503–516, DOI: 10.1007/s00382-006-0200-2.

Lewis, M. R., M. E. Carr, G. C. Feldman, W. Esias, and C. McClain, 1990: Influence of penetrating solar radiation on the heat budget of the equatorial Pacific Ocean. *Nature*, **347**, 543–545.

Lin, P. F., H. L. Liu, and X. H. Zhang, 2007: Sensitivity of the upper ocean temperature and circulation in the equatorial Pacific to solar radiation penetration due to phytoplankton. *Adv. Atmos. Sci.*, **24**, 765–780.

Liu, H. L., Y. Q. Yu, W. Li, and X. H. Zhang, 2004a: *Manual for LASG/IAP Climate System Ocean Model* (*LICOM1.0*). Science Press, Beijing, 1–128. (in Chinese)

Liu, H. L., X. H. Zhang, W. Li, Y. Q. Yu, and R. C. Yu, 2004b: A eddy-permitting oceanic general circulation model and its preliminary evaluations. *Adv. Atmos. Sci.*, **21**, 675–690.

Manizza, M., C. Le Quéré, A. J. Watson, and E. T. Buitenhuis, 2005: Bio-optical feedbacks among phytoplankton, upper ocean physics and sea-ice in a global model. *Geophys. Res. Lett.*, **32**, L05603, doi: 10.1029/2004GL020778.

Marzeion, B., A. Timmermann, R. Murtugudde, and F. F. Jin, 2005: Bio-physical feedbacks in the tropical Pacific. *J. Climate*, **18**, 58–70.

Mechoso, C. R., and Coauthors, 1995: The seasonal cycle over the tropical Pacific in coupled ocean-atmosphere general circulation models. *Mon. Wea. Rev.*, **123**, 2825–2838.

Miller, A. J., and Coauthors, 2003: Potential feedbacks between Pacific Ocean ecosystems and interdecadal climate variations. *Bull. Amer. Meteor. Soc.*, **84**, 617–633.

Murtugudde, R., J. Beauchamp, C. R. McClain, M. Lewis, and A. J. Busalacchi, 2002: Effects of penetrative radiation on the upper tropical ocean circulation. *J. Climate*, **15**, 470–486.

Nakamoto, S., S. P. Kumar, J. M. Oberhuber, J. Ishizaka, K. Muneyama, and R. Frouin, 2001: Response of the equatorial Pacific to chlorophyll pigment in a mixed layer isopycnal ocean general circulation model. *Geophys. Res. Lett.*, **28**(10), 2021–2024.

Ohlmann, J. C., D. A. Siegel, and L. Washburn, 1998: Radiant heating of the western equatorial Pacific during TOGA-COARE. *J. Geophys. Res.*, **103**, 5379–5395.

Ohlmann, J. C., 2003: Ocean radiant heating in climate models. *J. Climate*, **16**, 1337–1351.

Pacanowski, R. C., and S. G. H. Philander, 1981: Parameterization of vertical mixing in numerical models of tropical oceans. *J. Phys. Oceanogr.*, **11**, 1443–1451.

Paulson, C. A., and J. J. Simpson, 1977: Irradiance measurements in the upper ocean. *J. Phys. Oceanogr.*, **7**, 952–956.

Röske, F., 2001: An atlas of surface fluxes based on the ECMWF Re-Analysis—A climatological dataset to force global ocean general circulation models. Report No. 323, MPI, Hamburg, 31pp.

Sathyendranath, S., A. D. Gouveia, S. R. Shetye, P. Ravindran, and T. Platt, 1991: Biological control of surface temperature in the Arabian Sea. *Nature*, **349**, 54–56.

Shell, K. M., R. Frouin, S. Nakamoto, and R. C. J. Somerville, 2003: Atmospheric response to solar radiation absorbed by phytoplankton. *J. Geophys. Res.*, **108**, 4445, doi: 10.1029/2003JD003440.

Siegel, D. A., J. C. Ohlmann, L. Washburn, R. R. Bidigare, C. Nosse, E. Fields, and Y. Zhou, 1995: Solar radiation, phytoplankton pigments and radiant heat-

ing of the equatorial Pacific warm pool. *J. Geophys. Res.*, **100**, 4885–4891.

Strutton, P., and F. P. Chavez, 2004: Biological heating in the equatorial Pacific: Observed Variability and Potential for Real-Time Calculation. *J. Climate*, **17**, 1097–1109.

Sweeney, C., A. Gnanadesikan, S. M. Griffies, M. J. Harrison, A. J. Rosati, and B. L. Samuels, 2005: Impacts of shortwave penetration depth on large-scale ocean circulation and heat transport. *J. Phys. Oceanogr.*, **35**, 1103–1119.

Timmermann, A., and F. F. Jin, 2002: Phytoplankton influences on tropical climate. *Geophys. Res. Lett.*, **29**, 2104, doi:10.1029/2002GL015434.

Wetzel, P., E. Maier-Reimer, M. Botzet, J. Jungclaus, N. Keenlyside, and M. Latif, 2006: Effects of ocean biology on the penetrative radiation in a coupled climate model. *J. Climate*, **19**, 3973–3987.

Wu, F., H. Liu, W. Li, and X. Zhang, 2005: Effect of adjusting vertical resolution on the eastern equatorial Pacific cold tongue. *Acta Oceanologica Sinica*, **24**, 1–12.

Zhang, X. H., Y. Q. Yu, and H. L. Liu, 2003: The Development and Application of the Oceanic Circulation Models, Part I. the Global Oceanic General Circulation Models. *Chinese Journal of Atmospheric Sciences*, **27**, 607–617. (in Chinese)